

Assessment of maize hybrid water status using aerial images from an unmanned aerial vehicle

Detecção do estado hídrico em híbridos de milho com imagens aéreas obtidas por aeronave remotamente pilotada

Alzeneide da S. Lopes^{1*} , Aderson S. de Andrade Júnior² , Edson A. Bastos² , Carlos A. F. de Sousa² ,
Raphael A. das C. N. Casari³ , Magna S. B. de Moura⁴ 

¹Postgraduate Program in Agronomy, Universidade Federal do Piauí, Teresina, PI, Brazil. ²Embrapa Meio-Norte, Teresina, PI, Brazil. ³Embrapa Agroenergia, Brasília, DF, Brazil. ⁴Embrapa Semiárido, Petrolina, PE, Brazil.

ABSTRACT - The objective of this work was to evaluate the potential of vegetation indices (VIs), obtained using aerial images from an unmanned aerial vehicle (UAV), for assessing water status of maize hybrids subjected to different water regimes under the soil and climate conditions of Teresina, Piauí, Brazil. Evaluations were carried out considering the application of five water regimes (WR) based on the crop evapotranspiration (ETc) (40%, 60%, 80%, 100%, and 120% of ETc) for three maize hybrids: BRS 3046 (conventional triple hybrid), BRS 2022 (conventional double hybrid), Status VIP3 (transgenic simple hybrid). A randomized block experimental design with four replications was used, in a 5×3 split-plot arrangement, consisting of WRs in the plots and maize hybrids in the subplots. A UAV was used for acquiring multispectral images. Eighteen VIs were evaluated and correlated with stomatal conductance (*gs*), leaf relative water content (RWC), and grain yield (GY). The VIs TCARI-RE and NDVI presented correlation with *gs*, whereas MNGRD and GCI presented correlation with RWC; therefore, they were considered promising for assessing the water status of maize plants. NDVI and WDRVI presented correlations with GY. Maps of NDVI, MNGRV, and WDRVI showed spatial correlation with *gs*, RWC, and GY measurements, respectively, in response to the applied WRs, denoting potential for assessing the water status of maize plants using aerial images from UAV.

Keywords: Drone. Cultivar. Water stress. Vegetation index. Remote sensing.

Conflict of interest: The authors declare no conflict of interest related to the publication of this manuscript.



This work is licensed under a Creative Commons Attribution-CC-BY <https://creativecommons.org/licenses/by/4.0/>

Received for publication in: January 29, 2023.
Accepted in: September 4, 2023.

***Corresponding author:**
<agro.neide@hotmail.com>

RESUMO - Objetivou-se avaliar a capacidade de índices de vegetação (IV), obtidos de imagens aéreas por aeronave remotamente pilotada (ARP), em detectar o estado hídrico de híbridos de milho submetidos a diferentes regimes hídricos, nas condições de solo e clima de Teresina, Piauí, Brasil. Avaliou-se a aplicação de cinco regimes hídricos (RHs) com base na evapotranspiração da cultura (ETc) (40%, 60%, 80%, 100% e 120% da ETc) em três híbridos de milho: BRS 3046 (híbrido triplo convencional); BRS 2022 (híbrido duplo convencional); e Status VIP3 (híbrido simples transgênico). O delineamento experimental foi o de blocos ao acaso, parcelas subdivididas, sendo as parcelas os RHs e as subparcelas os híbridos, com quatro repetições. Utilizou-se uma ARP para a aquisição das imagens multiespectrais. Avaliaram-se 18 índices de vegetação, os quais foram correlacionados com medidas de condutância estomática (*gs*), conteúdo relativo de água na folha (CRA) e produtividade de grãos (PG). Os IVs TCARI-RE e NDVI apresentaram correlação com *gs* e os IVs MNGRD e GCI foram correlacionados com o CRA e, portanto, são considerados promissores na detecção do estado hídrico do milho. Os IVs NDVI e WDRVI apresentaram correlações com a PG. Os mapas de NDVI, MNGRV e WDRVI mostraram correlação espacial com as medidas de *gs*, CRA e PG, respectivamente em resposta aos RHs, indicando aplicação potencial na detecção do estado hídrico do milho por meio de imagens aéreas obtidas por ARPs.

Palavras-chave: Drone. Cultivar. Estresse hídrico. Índice de vegetação. Sensoriamento remoto.

INTRODUCTION

Water is one of the limiting factors for maize grain yield (BERGAMASCHI; MATZENAUER, 2014). Soil water deficit changes physiological responses in plants and can negatively affect growth and yield when lasting for a long time (OSAKABE et al., 2014). In the case of maize plants, water stress has been associated with decreases in stomatal conductance and photosynthesis.

Traditional methods for monitoring water stress in crops include direct measurements of soil water content and direct and indirect measurements of plant physiological variables, such as stomatal conductance and leaf water potential (IHUOMA; MADRAMOOTOO, 2017). However, these are time-consuming, laborious, and costly methods that do not consider the spatial variability of soil and crops (LI et al., 2010).

In this sense, remote sensing techniques using aerial images acquired by satellites or drones are recommended as alternatives, providing several advantages over traditional methods of monitoring water stress in the field.

In this context, the use of unmanned aerial vehicles (UAVs) is an innovative and potential method for monitoring and quantifying water in different

cropping systems compared to traditional water stress monitoring methods (HOGAN et al., 2017; HUNT; DAUGHTRY, 2018), as it is a fast and non-destructive method for managing water stress in plants through measurements of spectral reflectance of crop canopies (JONES; VAUGHAN, 2010). Moreover, it provides information on the spatial and temporal variability of crops (ROSSINI et al., 2015; PANIGADA et al., 2014; BALLESTER et al., 2019; ZHANG et al., 2021).

Vegetation indices from spectral information can be used for a rapid and efficient assessment of crop water status and crop yields through remote sensing techniques. Studies have shown that vegetation indices from aerial images taken by UAVs can be used for estimating leaf water potential and mapping water status variability in agricultural crops (BAJULA et al., 2012; ZHANG et al., 2021; ANDRADE JUNIOR et al., 2021).

Assessing water stress in crops during the initial stage is essential for farmer's decision-making and contributes to preventing decreases in crop yields. Remote sensing data obtained through cameras attached to UAV assist in a rapid and accurate management production of maize crops.

Therefore, the objective of this work was to evaluate the potential of vegetation indices (VI), obtained using aerial images from an unmanned aerial vehicle (UAV), for assessing water status of maize hybrids subjected to different water regimes under the soil and climate conditions of Teresina, Piauí, Brazil.

MATERIAL AND METHODS

The study was conducted at the experimental area of the Brazilian Agricultural Research Corporation (EMBRAPA Mid-North) (05°05'S, 42°48'W, and 74.4 m of altitude), in Teresina, PI, Brazil, from August to November 2019. The climate of region was classified as Aw, with a wet summer and a dry winter (MEDEIROS; CAVALCANTI; DUARTE, 2020). The mean annual air temperature and rainfall depth are 27.4 °C and 1,325 mm, respectively, with rainfalls concentrated from January to May. The mean maximum and minimum temperatures and accumulated rainfall depth during the experimental period were 29.4 °C, 27.2 °C, and 18.6 mm, respectively. The maximum and minimum temperatures, wind speed, and global solar radiation at the time of the UAV flight (11:00 am to 12:00 pm) were 30.7 °C, 29.3 °C, 2.8 m s⁻¹, and 406.8 W m⁻², respectively (INMET, 2020).

The soil of the experimental area was classified as a Typic Hapludult (Argissolo Vermelho-Amarelo Distrófico típico; Santos et al., 2018), whose chemical and physical-hydrological characteristics are shown in Table 1. The soil was prepared in a conventional system, with one plowing and two harrowing. Soil fertilizers were applied at sowing, using 75 kg ha⁻¹ of N, 80 kg ha⁻¹ of P₂O₅, 35 kg ha⁻¹ of K₂O, and 3 kg ha⁻¹ of Zn. Topdressing was carried out when the plants had 6 fully expanded leaves, using 75 kg ha⁻¹ of N and 35 kg ha⁻¹ of K₂O. The fertilizer sources were ammonium sulfate (N), triple superphosphate (P₂O₅), potassium chloride (K₂O), and zinc sulfate (Zn).

Table 1. Chemical and physical-hydrological characterization of the soil in the experimental area.

Layer (m)	OM	pH	P	K	Mg	Ca	Na	CEC	BS
	g kg ⁻¹	H ₂ O	mg dm ⁻³			cmolc dm ⁻³			%
0.0-0.2	12.9	5.78	31.12	0.09	0.35	0.78	0.02	2.94	42.32
0.2-0.4	11.2	5.95	23.49	0.09	0.42	0.73	0.02	2.89	44.11
Layer (m)	Density (g cm ⁻³)	Sand			Silt		Clay	Θ _{cc}	Θ _{mp}
		-----g kg ⁻¹ -----						(%, volume)	
0.0-0.2	1.70	876.5			37.5		86.0	21.7	5.3
0.2-0.4	1.65	811.5			52.5		136.0	20.8	6.0

Laboratory of Soils at the Brazilian Agricultural Research Corporation (EMBRAPA Mid-North). OM = organic matter; CEC: cation exchange capacity; BS = base saturation; Θ_{cc} = moisture at field capacity; Θ_{mp} = moisture at the permanent wilting point.

The experiment was conducted under irrigation, using a conventional fixed sprinkler system, with sprinklers spaced at 12×12 m. Irrigations were carried out on Mondays, Wednesdays, and Fridays, considering the ET_c of the period, according to the water regime treatments. The applications of five water regimes (WR) were evaluated as a function of the crop evapotranspiration (ET_c) (40%, 60%, 80%, 100%, and 120% of ET_c), using three maize hybrids: BRS 3046 (conventional triple hybrid), BRS 2022 (conventional double hybrid), and Status VIP3 (transgenic simple hybrid). The different WRs were applied using different irrigation times.

The Penman-Monteith method was used for estimating the reference evapotranspiration (ET_o) and crop coefficients (K_c) (ALLEN et al., 1998).

The following irrigation managements were used for applying the WRs: full irrigation was applied to all treatments (vegetative development stage) from sowing until 36 days after sowing (DAS); the differentiated WRs were applied from 37 DAS to the end of the crop cycle by applying 40%, 60%, 80%, 100%, and 120% of ET_c. Table 2 shows the irrigation water depths applied from sowing until the date of aerial images capture and the total irrigation for each WR.

Table 2. Irrigation water depths (mm) applied to maize hybrids as a function of water regimes, from sowing (S) until the date of aerial images capture (September 24, 2019) and until the end of the crop cycle.

Period	DAS	40% ETc	60% ETc	80% ETc	100% ETc	120% ETc
Aug 05 to Sep 09, 2019	0–36	184.0	184.6	186.4	182.1	179.3
Sep 10 to Sep 24, 2019*	37–50	37, 2	57.0	74.2	91.6	108.8
Sep 25 to Nov 12 2019**	51– 99	114.8	165.2	210.7	272.3	330.5
Total	0–99	336.0	406.8	471.3	546.0	618.6

DAS = days after sowing; *The rainfall depth in the period was 5.2 mm; **The rainfall depth in the period was 13.4 mm.

Soil water content (% volume) was monitored using three PVC access tubes installed at each WR treatment at a depth of 0.7 m, arranged between central rows. A capacitance probe (FDR; Diviner 2000[®], Sentek Pty, Australia) was used. Readings were taken daily, both before and approximately 24 hours after irrigation events. The soil water content in each layer (0.10, 0.20, 0.30, and 0.40 m) of each WR treatment was calculated based on the mean moisture measured throughout the maize cycle.

A randomized block experimental design with four replications was used, in a 5×3 split-plot arrangement, consisted of WRs in the plots and maize hybrids in the subplots. Sowing was carried out with spacing of 0.5 m between rows, using four plants per meter (8 plants per square meter). The plot was composed of six rows; the two central rows (6 m²) were used for evaluating grain yield. The seeds were sown on August 05, 2019. Harvesting was based on the physiological maturity of grains for the water regimes and occurred on November 12, 2019 (99 DAS).

Stomatal conductance (*g_s*) and leaf relative water content (RWC) were measured on the same day as the aerial images were captured; *g_s* was measured using a portable gas analyzer (CIRAS-3; PP Systems, Amesbury, USA) in the infrared electromagnetic spectrum region. Measurements were taken on one plant per subplot when the plants were at the culm elongation/pre-flowering stage, focusing on the youngest fully expanded leaf.

Leaf samples were collected for evaluating RWC, considering the first fully expanded leaf from the plant's apex. RWC was obtained using a sample of approximately 4.9 cm² of leaf blade from one plant per subplot. The samples were immediately placed in a hermetically closed container with a known weight to prevent water loss by transpiration. Fresh matter was weighed, and the samples were individually placed in Petri dishes with filter paper saturated with distilled water, where they remained for 24 hours under these conditions; the turgid weight was then determined. The dry weight of the samples was obtained after drying the materials in an oven at 65 °C until constant weight. RWC was calculated using Equation 1.

$$RWC(\%) = \frac{FW - DW}{(TW - DW)} \times 100 (\%) \quad (1)$$

Where *RWC* is the leaf relative water content, *FW* is the fresh weight of the sample (g), *TW* is the turgid weight of the sample (g), and *DW* is the dry weight of the sample (g).

Aerial images were taken using an unmanned aerial vehicle (UAV), specifically a hexacopter type, (X800; XFly Brazil, Bauru, Brazil). A flight was conducted on September 24, 2019 (50 DAS), between 11:00 am and 12:00 pm. The flight plan was developed using the software Pix4D Capture[®] (www.pix4d.com). The flight plan was created to ensure that images were taken with 80% lateral and frontal overlaps, maintaining the flight altitude at 30 meters above ground level, with a ground sample distance of ≈ 1.5 cm.

Multispectral images were acquired by a multispectral sensor (RedEdge; MicaSense, Seattle, USA). The sensor captures images in five narrow spectral bands: Blue (B; range: 465–485 nm; width: 20 nm), Green (G; range: 550–570 nm; width: 20 nm), Red (R; range: 663–673nm; width: 10 nm), Red Edge (range: 712–722 nm; width: 10 nm), and Near-Infrared (NIR) (range: 820–860 nm; width: 40 nm), with pixels ranging from 8 cm to 12 cm and resolution of 1280 × 960 pixels for each band. The images were saved in 16-bit TIFF format.

The obtained images underwent radiometric calibration, using a specific calibration target for the camera and radiation sensor mounted on top of the UAV. The processing to generate an orthomosaic of the aerial images was performed using the software OpenDroneMap Web version (WebODM) (TOFFANIN, 2019). The software configuration enabled the generation of an orthomosaic with spatial resolution of 4.6 cm.

The orthomosaic was subjected to a supervised classification process (maximum likelihood method), enabling the rasterization of the orthomosaic into two classes (soil and leaves); this step allowed for the removal of pixels classified as soil from the mosaic, ensuring that vegetation indices were estimated only with pixels classified as leaves. This processing step was conducted using the Semi-Automatic Classification (SCP) plugin in the QGIS v. 2018.

Sixteen vegetation indices were evaluated through estimates from the bands of the multispectral images (R, G, B, Red Edge, and NIR). Table 3 provides a description of the indices used, including their names, abbreviations, equations, and bibliographic references.

Table 3. Description of the evaluated multispectral vegetation indices.

Vegetation index	Equation Mathematical	Reference
Green chlorophyll index	$GCI = \frac{R_n}{R_g} - 1$	Gitelson et al. (2005)
Modified excess green	$MEXG = 1.262R_g - 0.884R_r - 0.311R_b$	Burgos-Artizzu et al. (2011)
Modified normalized green red difference	$MNGRD = \frac{R_g^2 - R_r^2}{R_g^2 + R_r^2}$	Bendig et al. (2015)
Normalized difference Red-Edge –	$NDRE = \frac{R_n - R_{RE}}{R_n + R_{RE}}$	Wang, Azzari and Lobell (2019)
Normalized difference Red-Edge index	$NDREI = \frac{R_{RE} - R_g}{R_{RE} + R_g}$	Hassan et al. (2018)
Normalized Difference Vegetation Index	$NDVI = \frac{R_n - R_r}{R_n + R_r}$	Gitelson et al. (2005)
Normalized green red difference –	$NGRD = \frac{R_g - R_r}{R_g + R_r}$	Hamuda, Glavin and Jones (2016)
Pigment-specific normalized difference index	$PSND = \frac{R_n - R_b}{R_n + R_b}$	Blackburn (1998)
Red-Edge chlorophyll index	$RECI = \frac{R_n}{R_{RE}} - 1$	Gitelson et al. (2005)
Red green difference –	$RGD = R_r - R_g$	Sanjerehei (2014)
Ratio vegetation index RVI	$RVI = \frac{R_n}{R_r}$	Tucker (1979)
Soil Adjusted Vegetation Index	$SAVI = \frac{1.5(R_n - R_r)}{(R_n + R_r + 0.5)}$	Zhong, Hu and Zhou (2019)
Transformed chlorophyll absorption in Nir index	$TCARI = 3[(R_{n'} - R_{r'}) - 0.2(R_{n'} - R_{g'})](R_{n'}/R_{r'})]$	Haboudane et al. (2002)
TCARI/OSAVI index	$TCARI - OSAVI = \frac{TCARI}{OSAVI}$	Haboudane et al. (2002)
Transformed chlorophyll absorption in Red-edge index	$TCARI - RE = 3 \left[(R_{RE} - R_r) - 0.2(R_{RE} - R_g) \left(\frac{R_{RE}}{R_r} \right) \right]$	Daughtry et al. (2000)
Wide dynamic range vegetation index	$WDRVI = \frac{(0.12R_n) - R_r}{(0.12R_n) + R_r}$	Gitelson (2004)

Spectral reflectance: R_n : near-infrared (840 nm); R_g : green (560 nm); R_{RE} : red edge (717 nm); R_r : red (668 nm) and R_b : blue (475 nm); $R_{n'}$: near-infrared (soil); $R_{r'}$: red (soil).

The multispectral indices were estimated using the QGIS raster calculator (QGIS, 2016). The vegetation indices for each subplot were extracted using the QGIS zonal statistics plugin (QGIS, 2016); the vector layer representing the experimental subplots, which were consisted of four

central rows (12 m²) containing only areas classified as leaves, was used in this process. The zonal statistics plugin generated an attribute table (minimum, maximum, and standard deviation) for the vegetation indices for each experimental subplot.

Manual harvesting was carried out on November 12, 2019 (dry grains), at 99 DAS. All maize ears in an area of 6 m² of each subplot, in the central rows of the subplots, were harvested to determine grain yield. The harvested ears were threshed using a thresher machine to obtain the grains. The weight of grains from each subplot was measured and corrected to a moisture content of 130 g kg⁻¹; the result was extrapolated to kg ha⁻¹.

The data were subjected to statistical analysis, according to the following strategy: a) analysis of variance to assess the response of physiological parameters (*gs* and RWC) and grain yield (GY) to the sources of variation: water regimes (WR), maize hybrids (H), and interaction (WR×H); b) Pearson's correlation analysis between *gs*, RWC, grain yield, and vegetation indices, focusing on the pre-selection of the most promising vegetation indices (VIs) for assessing the water status of maize plants; c) linear regression analysis to generate prediction models for *gs*, RWC, and GY, using the promising VIs for assessing the water status of maize plants.

The t-test was applied for Pearson's correlation analysis (*r*), and the F test was used for analysis of variance of the factors WR, H, and WR×H. Promising VIs were those with *r* ≥ 0.8 regarding the parameters *gs*, RWC, and GY. The statistical analyses were conducted using the ExpDes.pt package of the R software (FERREIRA; CAVALCANTI; NOGUEIRA, 2014). The linear regression models were selected considering the coefficient of determination (R²) and the standard error of the regression (SER), according to Equation 2 and Equation 3, respectively; those with higher R² and lower SER were considered the best regression models.

$$R^2 = \frac{\sum_{i=1}^n (\hat{Y}_i - \bar{Y}_m)^2}{\sum_{i=1}^n (Y_i - \bar{Y}_i)^2} \tag{2}$$

$$SER = \sqrt{\frac{\sum_{i=1}^n (Y_i - \hat{Y}_i)^2}{n - 2}} \tag{3}$$

Where *n* is the number of observations, \hat{Y}_i is the parameter estimated by the regression models, \bar{Y}_m is the mean of the parameters estimated by the regression models, Y_i is the parameter measured in the field, and \bar{Y}_i is the mean of the physiological parameters measured in the field.

RESULTS AND DISCUSSION

The evaluated water regimes (WR) resulted in variations in soil water availability to maize plants; soil water availability was higher when higher water depths were applied. The variability was higher in the 0.0-0.1 and 0.1-0.2 m soil layers (Figure 1). Regarding the total evaluated soil layer (0.0-0.4 m), the means of soil moisture ranged from 7.1% (WR = 40% of ETc) to 15.4% (WR = 120% of ETc) (Figure 1A), resulting in a mean variation in soil water availability from 45.0% (WR = 40% of ETc) to 98.1% (WR = 120% of ETc) (Figure 1B).

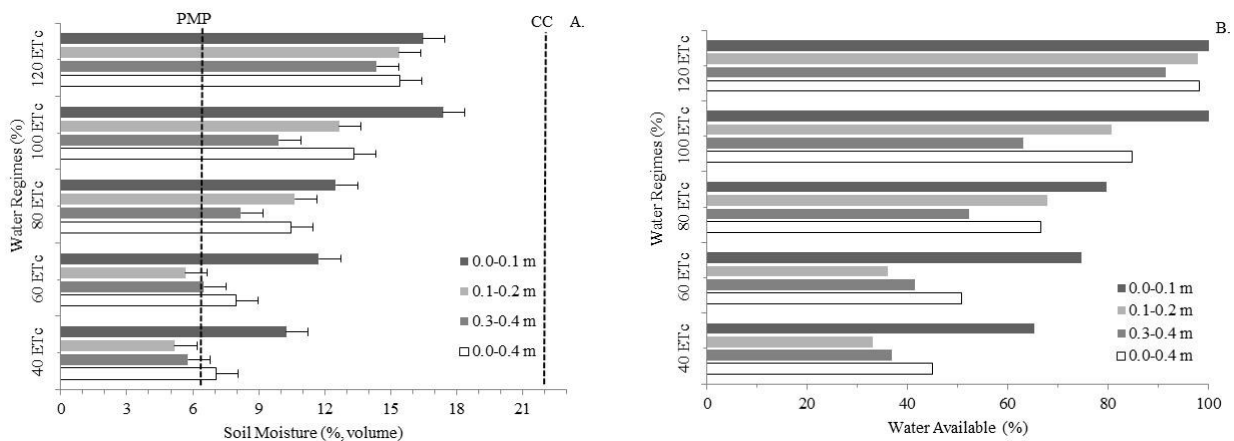


Figure 1. Soil moisture (A) and soil water available (B) as a function of the water regimes applied from maize sowing until the date of aerial image acquisition (September 24, 2019).

The soil water availability in the 0.0-0.4 soil layer in the treatments under WRs of 80% (10.5%), 100% (13.3%), and 120% of ETc (15.4%) was maintained at levels higher than the critical moisture level (the mean of the 0.0-0.4 soil layer was 10.8%), allowing for adequate maize plant development and production. However, treatments under WRs of 40% (7.1%) and 60% of ETc (8.0%) presented soil water availability below the critical moisture level (50%) (DOORENBOS; KASSAM, 1994) and above the permanent

wilting point during the evaluated period, which is a limiting factor for maize development and grain yield.

The analysis of variance indicated significant changes in the parameters stomatal conductance (*gs*), leaf relative water content (RWC), and grain yield (GY) in response to WR applications. The effect of maize hybrid (H) and the interaction between WR and H was significant (*p* < 0.001) only for GY (Table 4).

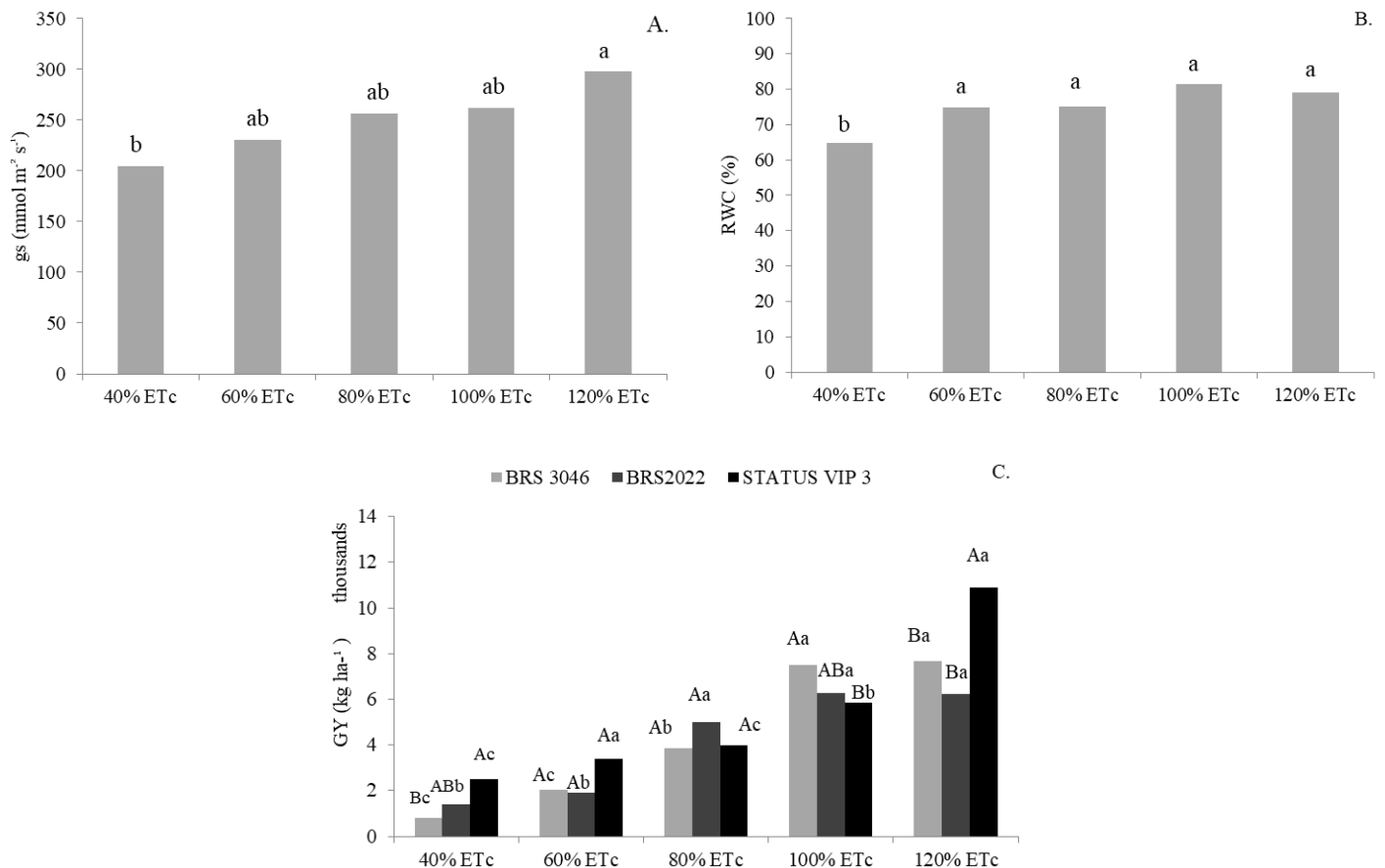
Table 4. Analysis of variance for stomatal conductance (g_s), leaf relative water content (RWC), and grain yield (GY) in response to the evaluated water regimes and maize hybrids.

Source of Variation	DF	g_s	RWC	GY
Water regime (WR)	4	14995*	490.940***	93362560***
Block	3	5371	80.110	3813255
Error a	12	3309	40.720	495152
Hybrid (H)	2	2211 ^{ns}	107.850 ^{ns}	7644094***
RH×H	8	7003 ^{ns}	28.410 ^{ns}	6402201***
Error b	30	4873	41.640	787322
Total	59			
CV WR (%)		22.97	8.50	15.23
CV H (%)		27.87	8.60	19.21

CV = coefficient of variation; DF = degrees of freedom; Significance levels by the F test: *** = $p < 0.001$; ** = $p < 0.01$; * = $p < 0.05$; and ns = not significant.

The increase in soil water availability as a function of WR application increased g_s (Figure 2A), mainly for the treatments under the extreme WRs (40% and 120% of ETc), which resulted in g_s of $204.2 \text{ mmol m}^{-2} \text{ s}^{-1}$ and $298.5 \text{ mmol m}^{-2} \text{ s}^{-1}$, respectively. The maize plants under WRs of 60%, 80%, and 100% of ETc presented no significant

differences in g_s . Similarly, Rossini et al. (2015), Zhang et al. (2021), and Andrade Junior et al. (2021) found decreased g_s in maize plants under soil water deficit. Stomatal closure is among the first responses of plants to water deficit as a strategy to avoid water loss to the atmosphere (ROSSINI et al., 2015).


Figure 2. Stomatal conductance (g_s), leaf relative water content (RWC), and grain yield (GY) of three maize hybrids in response to the application of five different water regimes. Teresina, PI, 2019. Means followed by the same letter are not significantly different from each other by the Tukey's test at 5% probability level. Lowercase letters (WR) and uppercase letters (hybrids).

RWC varied under conditions of high soil water availability, ranging from 79.0% (120% of ETc) to 81.5% (100% of ETc), whereas it decreased to 64.7% in the treatment under 40% of ETc (Figure 2B). However, maize plants subjected to treatments under 60%, 80%, 100%, and 120% of ETc presented no significant difference in RWC. Decreased RWC in maize plants under soil water restriction conditions was also found by Rossini et al. (2015).

RWC can directly affect the actual growth and development status of crops, which makes it the best parameter for assessing the water conservation status of leaves. According to Xingyang et al. (2020), changes in RWC are easily observed and can indicate the degree of plant stress to some extent, as the leaf is the most important organ for assimilation and transpiration in plants, making it the most sensitive to water stress.

Regarding GY, higher means were found under high soil water availability conditions (100% and 120% of ETc) compared to those found in treatments under 40%, 60%, and 80% of ETc; therefore, GY was lower under soil water deficit conditions (Figure 2C). The highest GY mean in the treatment under 120% of ETc was found for the maize hybrid VIP3 (10,898.3 kg ha⁻¹), differing from the hybrids BRS 3046 and BRS 2022, which were statistically similar and presented the lowest GY (7,653.8 and 6,214.5 kg ha⁻¹, respectively). VIP3

also had the highest GY under water deficit conditions (40% and 60% of ETc), differing statistically from the other hybrids.

The soil water availability level directly affects maize grain yield. Elmetwalli and Tyler (2020) reported that water stress significantly reduced GY. They found the highest GY (8.4 and 9.4 Mg ha⁻¹) with application of a water depth corresponding to 125% ETc replacement in the 2015 and 2016 crop seasons, respectively. Considering the present study, the WR with 120% ETc replacement corresponded to a total of 618.6 mm (Table 2).

All evaluated vegetation indices, except RGD, showed a significant effect (0.05 ≤ p ≤ 0.001) of the applied WRs (Table 5). This result denotes that the most significant vegetation indices by the F test have the potential for assessing the water status of maize plants. However, the promising vegetation indices selected were those that showed the best levels of correlation with the *gs*, RWC, and GY measurements obtained in the field. Regarding the evaluated maize hybrids, a significant effect was found for the vegetation indices GCI, MEXG, MNGRD, NDRE, NGRD, TCARI, TCARI-OSAVI, TCARI-RE, and WDRVI (0.01 ≤ p ≤ 0.001). However, the interaction effect between WR and H was found only for the index MEXG (p ≤ 0.05).

Table 5. F test for vegetation indices (VI) in response to water regimes (WR), maize hybrids (H), and interaction between WR and H (WR×H).

VI	WR	H	WR×H	VI	WR	H	WR×H
GCI	*	**	ns	RECI	***	ns	ns
MEXG	*	***	*	RVI	***	ns	ns
MNGRD	*	**	ns	SAVI	***	ns	ns
NDRE	***	***	ns	TCARI	***	***	ns
NRDEI	*	ns	ns	TCARI-OSAVI	***	***	ns
NDVI	**	ns	ns	RGD	ns	ns	ns
NGRD	*	***	ns	TCARI-RE	**	***	ns
PSND	***	ns	ns	WDRVI	***	**	ns

Significance levels by the F test: *** = p < 0.001; ** = p < 0.01; * = p < 0.05; and ns = not significant.

Stomatal conductance (*gs*) showed significant correlations with several vegetation indices, among which those resulting in correlations $r \geq 0.8$ were considered promising for assessing water status of maize plants (BALLESTER et al., 2019; ELMETWALLI; TYLER, 2020). Therefore, the indices NDVI ($r=0.946$; $p<0.01$), TCARI-RE ($r=-0.928$; $p<0.01$), WDRVI ($r=0.919$; $p<0.01$), and PSND ($r=0.908$; $p<0.01$) (Table 6) stood out. Studies have indicated that vegetation indices using spectral bands with wave lengths in the NIR region are more suitable for assessing the water status of crops under water stress conditions (ELSAIED; RISCHBECK; SCHMIDHALTER, 2015). In the present study, the indices that met this condition established by Elsayed, Rischbeck, and Schmidhalter (2015) were NDVI, PSND, and WDRVI. Additionally, TCARI-RE which uses spectral bands in the visible region (RGB) also was suitable

for assessing the water status of maize crops in the present study.

RWC showed significant correlation with several of the evaluated vegetation indices, among which GCI ($r=-0.920$; $p<0.01$), MNGRD ($r=0.925$; $p<0.01$), and NGRD ($r=0.916$; $p<0.01$) were considered promising for assessing RWC in maize leaves (BALLESTER et al., 2019; ELMETWALLI; TYLER, 2020), mainly the latter two indices, which use spectral bands in the RGB region.

GY showed significant correlations with most of the evaluated vegetation indices, with coefficients of correlation varying from 0.894 to 0.949 (Table 6). Evaluating correlations between crop vegetation indices and yield is important, as it is possible to predict crop yield in a simple, rapid, inexpensive, and non-destructive way when correlations are found (HOYOS-VILLEGAS; FRITSCHI, 2013).

Table 6. Pearson's correlation between vegetation indices (VI) and stomatal conductance (*gs*), leaf relative water content (RWC), and grain yield (GY) of maize hybrids.

VI	<i>gs</i>	RWC	GY	VI	<i>gs</i>	RWC	GY
GCI	-0.860**	-0.920**	-0.62ns	RDVI	0.722 ^{ns}	0.563 ^{ns}	0.911**
MEXG	-0.479 ^{ns}	-0.214 ^{ns}	-0.737 ^{ns}	RVI	0.882**	0.740 ^{ns}	0.949**
MNGRD	0.872**	0.925**	0.635 ^{ns}	SAVI	0.720 ^{ns}	0.557 ^{ns}	0.909**
NDRE	0.796 ^{ns}	0.603 ^{ns}	0.923**	TCARI	-0.798 ^{ns}	-0.627 ^{ns}	-0.927**
NDREI	0.169 ^{ns}	0.394 ^{ns}	0.487 ^{ns}	TCARI-OSAVI	-0.816**	-0.653 ^{ns}	-0.934**
NDVI	0.946**	0.875**	0.928**	TCARI-RE	-0.928**	-0.861**	-0.939**
NGRD	0.877 ^{ns}	0.916**	0.640 ^{ns}	RGD	-0.026 ^{ns}	-0.254 ^{ns}	0.288 ^{ns}
PSND	0.908**	0.803 ^{ns}	0.920**	WDRVI	0.919**	0.813**	0.948**

Significance levels by the t test: ** = $p < 0.01$; * = $p < 0.05$; ns = not significant.

The indices MEXG, NDREI, and RGD were not correlated with any of the field-measured parameters; the coefficients of correlation ranged from -0.214 to 0.949.

Exclusively, the correlations between vegetation indices and *gs*, RWC, and GY that presented the highest R^2 values are shown in Figure 3 for clarity purposes.

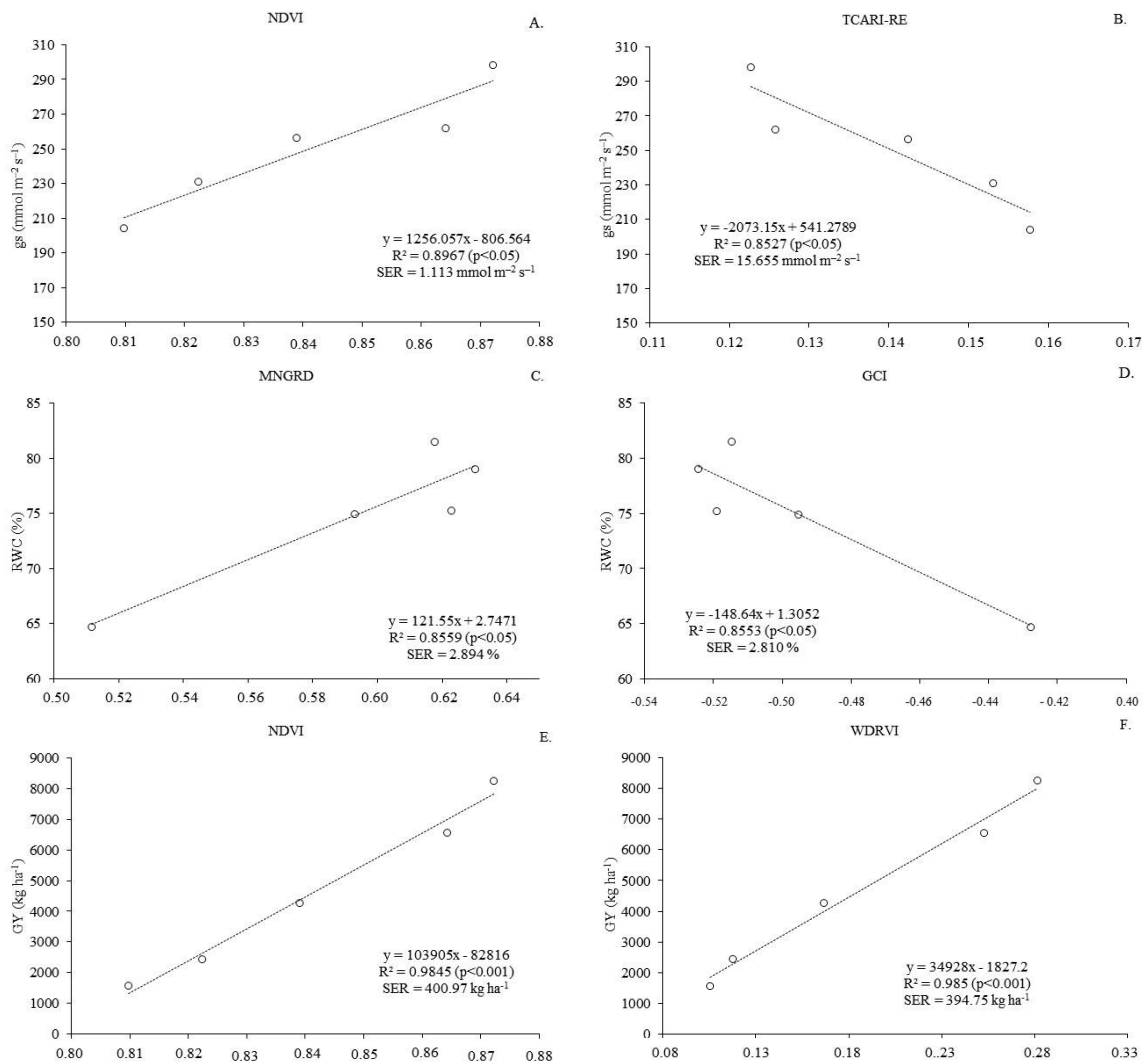


Figure 3. Linear regression models for stomatal conductance (*gs*) (A, B), leaf relative water content (RWC) (C, D), and grain yield (GY) (E, F) of maize hybrids based on the most promising vegetation indices. Significance levels by the t test: ns = not significant; * = $p < 0.05$; ** = $p < 0.01$; and *** = $p < 0.001$.

NDVI and TCARI-RE provided the best estimates of g_s , with R^2 ranging from 0.8527 ($p < 0.05$) to 0.8967 ($p < 0.05$) and standard error of the regression (SER) ranging from 13.113 $\text{mmol m}^{-2} \text{s}^{-1}$ to 15.655 $\text{mmol m}^{-2} \text{s}^{-1}$ (Figures 3A and 3B). This low error denotes that the use of NDVI and TCARI-RE is suitable for assessing water stress. Zhang et al. (2021) evaluated responses of maize plants to water stress by changes in canopy structure (leaf area) and chlorophyll content based on VI from multispectral images obtained by UAV. They found a significantly positive correlation between NDVI and g_s , with r values of 0.61 and 0.64 ($p < 0.001$), respectively; however, no significant correlation was found between TCARI-RE and g_s .

The indices MNGRD and GCI provided the best estimates of RWC, with R^2 of 0.855 ($p < 0.05$) and SER of 2.81% (Figures 3C and 3D). These vegetation indices presented sensitivity to RWC in terms of higher R^2 and lower SER. Increases in soil water availability promoted increases in RWC, which increased NDVI values. Contrastingly, treatments with higher water availability (100% and 120% of ETc) resulted in decreased GCI values while the parameter RWC increased. Therefore, the indices MNGRD (RGB) and GCI (NIR) presented correlations with the applied water

regimes and, consequently, with RWC.

NDVI and WDRVI provided the best estimates of GY, with R^2 of 0.98 ($p < 0.001$) and SER ranging from 394.75 to 400.97 kg ha^{-1} (Figures 3E and 3F). A positive linear increase in GY was found as the NDVI and WDRVI values increased. Therefore, soil water availability was determinant for increasing maize grain yield, with adequate water availability to plants grown under the best water conditions (100% and 120% of ETc).

Considering that the indices NDVI, MNGRD, and WDRVI showed the best correlations with g_s , RWC, and GY measured in the field, spatial variability maps of g_s , RWC, and GY were developed only for these indices. Thus, the spatial variability of g_s , RWC, and GY, generated with the indices that performed best in estimating these parameters in response to WRs (40%, 80%, and 120% of ETc), is shown in Figure 4. These indices allowed for mapping and differentiating maize plants under intense water stress from those without water stress, showing significant differences in g_s , RWC, and GY means. The other tested vegetation indices presented lower efficiency in assessing and separating maize plants based on their level of water stress.

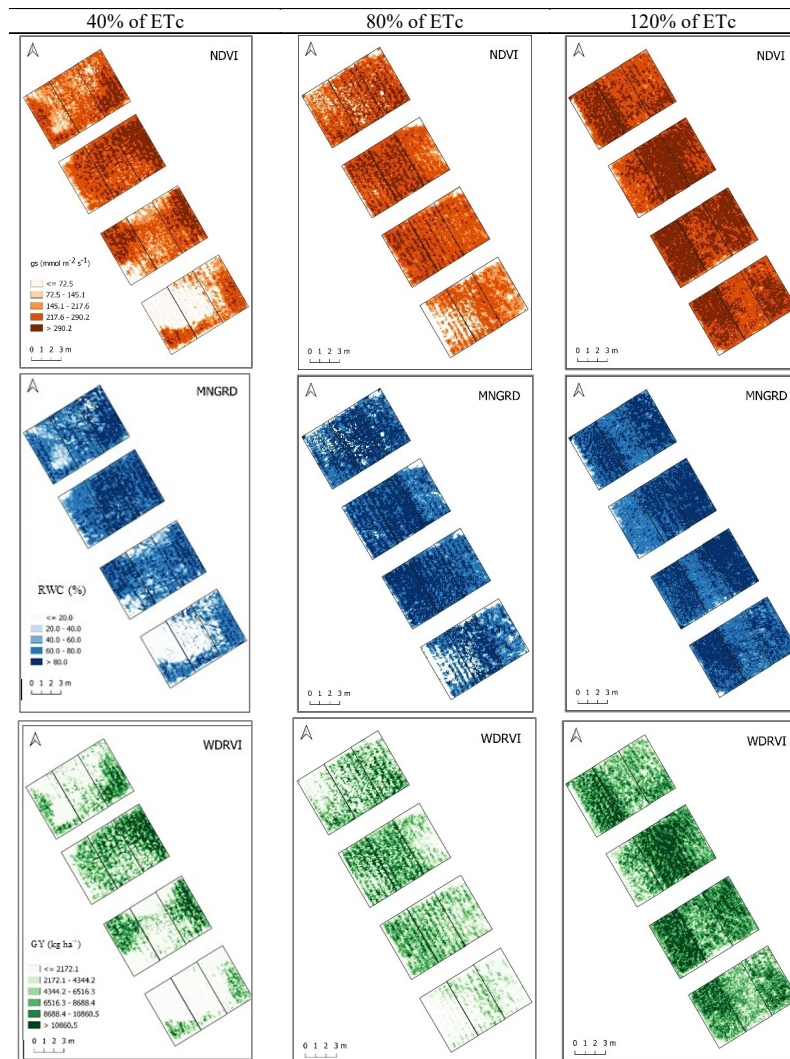


Figure 4. Maps of stomatal conductance (g_s), leaf relative water content (RWC), and grain yield (GY) based on the vegetation indices with better statistical performance.

The g_s maps highlights maize plants with more intense water stress through a lighter color on their canopy (Figure 4). Additionally, it was possible to identify plants with intermediate hue, denoting a moderate water stress. The g_s maps for the WRs of 40% and 80% of ETc showed areas with a higher predominance of zones with g_s below the range of 145.1 to 217.6 $\text{mmol m}^{-2} \text{s}^{-1}$, whereas the map for 120% of ETc showed areas with a higher predominance of g_s above the range of 217.6 to 290.2 $\text{mmol m}^{-2} \text{s}^{-1}$ (Figure 4), indicating lower spatial variability of g_s .

According to the maps, RWC was mainly concentrated in the range of 40% to 60% under 40% of ETc. The maps for 80% and 120% of ETc showed areas with a higher predominance of RWC above the range of 60% to 80%, indicating almost no water stress in these treatments. RWC is the best parameter to assess water status in leaves.

Changes in RWC are easily observed and can indicate the degree of water deficit in plants to some extent. Thus, RWC has an important function in assessing water stress in crops, mainly in remote sensing for water stress monitoring (ULLAH et al., 2012; ZHAO et al., 2016). Decreases in RWC can lead to increases in leaf temperature, which can cause stomatal closure and decreases in the net photosynthetic rate (XINGYANG et al., 2020). The comparison of g_s (NDVI) and RWC (MNGRD) maps clearly showed that zones with the lowest g_s and RWC are concentrated in the same parts of the experimental area, indicating the potential of these vegetation indices for detecting the water status of maize plants, mainly MNGRD, which uses spectral bands in the RGB region.

Regarding the spatial variability maps for GY, the means were distributed mainly in the range of 2,171.1 to 4,344.2 kg ha^{-1} under 40% of ETc, whereas the map for 80% of ETc showed areas with a higher predominance of GY in the range of 4,344.2 to 6,516.3 kg ha^{-1} . Regarding the map for 120% of ETc, the GY means concentrated mainly in the range of 8,688.4 to 10,860.5 kg ha^{-1} .

CONCLUSIONS

Increases in soil water availability promotes increases in stomatal conductance, leaf relative water content, and grain yield for maize plants.

The vegetation indices NDVI, TCARI-RE, MNGRD, and GCI are promising for assessing water status of maize plants, whereas NDVI and WDRVI are promising for estimating maize grain yield.

The maps generated using the indices NDVI, MNGRD, and WDRVI showed a significant spatial correlation with stomatal conductance, leaf relative water content, and grain yield, respectively, in response to the applied water regimes. These vegetation indices can be applied to aerial images from unmanned aerial vehicle for assessing water status of maize plants under field conditions.

REFERENCES

ALLEN, R. G. et al. **Crop evapotranspiration: Guidelines for computing crop water requirements**. Rome: FAO, 1998. 300 p. (Drainage and Irrigation Paper, 56).

ANDRADE JUNIOR, A. S. et al. Water status evaluation of maize cultivars using aerial images. **Revista Caatinga**, 34: 432-442, 2021.

BALLESTER, C. et al. Monitoring the effects of water stress in cotton using the green red vegetation index and red edge ratio. **Remote Sensing**, 11: 1-21, 2019.

BAJULA, J. et al. Assessment of vineyard water status variability by thermal and multispectral imagery using an unmanned aerial vehicle (UAV). **Irrigation Science**, 30: 511-522, 2012.

BENDIG, J. et al. Combining UAV-based plant height from crop surface models, visible, and near infrared vegetation indices for biomass monitoring in barley. **International Journal of Applied Earth Observation and Geoinformation**, 39: 79-87, 2015.

BERGAMASCHI, H.; MATZENAUER, R. **O milho e o clima**. Porto Alegre, RS: Emater/RS-Ascar, 2014. 84 p.

BLACKBURN, G. A. Quantifying chlorophylls and carotenoids at leaf and canopy scales: an evaluation of some hyperspectral approaches. **Remote Sensing of Environment**, 66: 273-285, 1998.

BURGOS-ARTIZZU, X. P. et al. Real-time image processing for crop/weed discrimination in maize fields. **Computers and Electronics in Agriculture**, 75: 337-346, 2011.

DAUGHTRY, C. S. T. et al. Estimating corn leaf chlorophyll concentration from leaf and canopy reflectance. **Remote Sensing of Environment**, 74: 229-239, 2000.

DOORENBOS, J.; KASSAM, A. H. **Efeito da água no rendimento das culturas**. Campina Grande, PB: UFPB, 1994. 306 p. (Estudos FAO: Irrigação e Drenagem, 33).

ELMETWALLI, A. H.; TYLER, A. N. Estimation of maize properties and differentiating moisture and nitrogen deficiency stress via ground-Based remotely sensed data. **Agricultural Water Management**, 242: 1-7, 2020.

ELSAYED, S.; RISCHBECK, P.; SCHMIDHALTER, U. Comparing the performance of active and passive reflectance sensors to assess the normalized relative canopy temperature and grain yield of drought stressed barley cultivars. **Field Crops Research**, 177: 148-160, 2015.

FERREIRA, E. B.; CAVALCANTI, P. P.; NOGUEIRA, D. A. ExpDes: an R package for ANOVA and experimental designs. **Applied Mathematics**, 5: 2952-2958, 2014.

GITELSON, A. A. et al. Remote estimation of canopy chlorophyll content in crops. **Geophysical Research Letters**, 32: 1-4, 2005.

GITELSON, A. A. Wide dynamic range vegetation index for remote quantification of biophysical characteristics of vegetation. **Journal of Plant Physiology**, 161: 165-173, 2004.

- HABOUDANE, D. et al. Integrated narrow-band vegetation indices for prediction of crop chlorophyll content for application to precision agriculture. **Remote Sensing of Environment**, 81: 416-426, 2002.
- HAMUDA, E.; GLAVIN, M.; JONES, E. A survey of image processing techniques for plant extraction and segmentation in the field. **Computers and Electronics in Agriculture**, 125: 184-199, 2016.
- HASSAN, M. A. et al. Time-series multispectral indices from unmanned aerial vehicle imagery reveal senescence rate in bread wheat. **Remote Sensing**, 10: 809-828, 2018.
- HOYOS-VILLEGAS, V.; FRITSCHI, F. B. Relationships among vegetation indices derived from aerial photographs and soybean growth and yield. **Crop Science**, 53: 2631-2642, 2013.
- HOGAN, S. et al. Unmanned aerial systems for agriculture and natural resources. **California Agriculture**, 71: 5-14, 2017.
- HUNT, E. R.; DAUGHTRY, C. S. T. What good are unmanned aircraft systems for agricultural remote sensing and precision agriculture?. **International Journal of Remote Sensing**, 39: 5345-5376, 2018.
- IHUOMA, S. O.; MADRAMOOTOO, C. A. Recent advances in crop water stress detection. **Computers and Electronics in Agriculture**, 141: 267-275, 2017.
- INMET - Instituto Nacional de Meteorologia. **Históricos de dados Meteorológicos**. Disponível em: <<https://portal.inmet.gov.br/dadoshistoricos>>. Acesso em: 30 nov. 2020.
- JONES, H. G.; VAUGHAN, R. A. **Remote sensing of vegetation: principles, techniques, and applications**. Oxford University Press, USA, 2010. 384 p.
- LI, L. et al. Evaluating the crop water stress index and its correlation with latent heat and CO₂ fluxes over winter wheat and maize in the North China plain. **Agricultural Water Management**, 97: 1146-1155, 2010.
- MEDEIROS, M. R.; CAVALCANTI, E. P.; DUARTE, J. F. M. Classificação climática de Köppen para o estado do Piauí-Brasil. **Revista Equador**, 9: 82-99, 2020.
- OSAKABE, Y. et al. Response of plants to water stress. **Frontiers in Plant Science**, 5: 81-88, 2014.
- PANIGADA, C. et al. Fluorescence, PRI and canopy temperature for water stress detection in cereal crops. **International Journal of Applied Earth Observation and Geoinformation**, 30: 167-178, 2014.
- QGIS Development Team. **QGIS User Guide, Release 2.18**: QGIS Project, 2016.
- ROSSINI, M. et al. Discriminating irrigated and rainfed maize with diurnal fluorescence and canopy temperature airborne maps. **ISPRS International Journal of Geo-Information**, 4: 626-646, 2015.
- SANJEREHEI, M. M. Assessment of spectral vegetation indices for estimating vegetation cover in arid and semiarid shrublands. **Range Management & Agroforestry**, 35: 91-100, 2014.
- SANTOS, H. G. et al. **Brazilian Soil Classification System**. 5. ed. Brasília, DF: Embrapa, 2018.
- TOFFANIN, P. **OpenDroneMap: The Missing Guide**. 1st ed. St Petersburg, Florida: UAV4GEO, 2019. 264 p.
- TUCKER, C. J. Red and photographic infrared linear combinations for monitoring vegetation. **Remote Sensing of Environment**, 8: 127-150, 1979.
- ULLAH, S. et al. An accurate retrieval of leaf water content from mid to thermal infrared spectra using continuous wavelet analysis. **Science of the Total Environment**, 437: 145-152, 2012.
- XINGYANG, S. et al. Stomatal limitations to photosynthesis and their critical Water conditions in different growth stages of maize under water stress. **Agricultural Water Management**, 241: 1-12, 2020.
- WANG, S.; AZZARI, G.; LOBELL, D. B. Crop type mapping without field-level labels: Random forest transfer and unsupervised clustering techniques. **Remote Sensing of Environment**, 222: 303-317, 2019.
- ZHANG, L. et al. Evaluating the sensitivity of water stressed maize chlorophyll and structure based on UAV derived vegetation indices. **Computers and Electronics in Agriculture**, 185, 1-9, 2021.
- ZHAO, S. et al. Estimating and validating wheat leaf water content with three MODIS spectral indexes: A case study in Ningxia Plain, China. **Journal of Agricultural Science and Technology**, 18: 387-398, 2016.
- ZHONG, L.; HU, L.; ZHOU, H. Deep learning based multi-temporal crop classification. **Remote Sensing of Environment**, 221: 430-443, 2019.